# 29. Pressuremeter measurement of total horizontal stress in stiff clay

P. G. HAWKINS, Cambridge Insitu, Cambridge, UK, R. J. MAIR, Geotechnical Consulting Group, London UK, W. G. MATHIESON, Merz Rendel Williamson, Glasgow, UK and D. MUIR WOOD, Glasgow University, Glasgow, UK

SYNOPSIS. Lift-off provides the most rational method for estimation of in situ total horizontal stress from pressuremeter tests in clay. An alternative method assumes elastic initial response of the clay and identifies a yield point from the cavity expansion information. Two examples are given of the application of both methods. At a London clay site the two methods produce similar results which agree reasonably well with estimates of in situ stress deduced from laboratory suction measurements. At a Barton clay site the two methods are used with results from both self-boring pressuremeter and high pressure dilatometer tests. Reasonable agreement is again obtained.

## INTRODUCTION

1. In an ideal cylindrical cavity expansion test the corrected data should indicate no radial movement at any point on the membrane until the cavity pressure reaches the in situ total horizontal stress. The moment of "lift-off", when radial movement begins, thus provides the only objective method of estimation of this in situ total horizontal stress, $\sigma_{ho}$. Lift-off will be a feasible technique with self-boring pressuremeter tests, where the pressuremeter has been installed with a minimum of disturbance but will certainly not be appropriate for tests where the pressuremeter is installed in a preformed borehole and where deformations of the soil will definitely have occurred before the cavity expansion is begun.

2. Alternatives to lift-off require some subjective statement about soil response for their justification. In this paper a combination of elastic and general analyses of undrained cavity expansion is used to construct a method by which in situ total horizontal stresses may be estimated from pressuremeter tests in stiff clays.

## THEORETICAL BACKGROUND

3. The analysis of the constant volume expansion of a long cylindrical cavity presented in Ref. 1 shows that, no matter what the material in which the cavity is being expanded (unless it exhibits rate dependent behaviour (Ref. 2)) the current slope of the cavity pressure $p:\ell n\ (\Delta V/V)$ curve is equal to the mobilised shear stress

$$\tau = (\sigma_r - \sigma_\theta)/2 = dp/d[\ell n(\Delta V/V)] \qquad (1)$$

The magnitude of the slope is dependent on the origin chosen for measuring the change in cavity volume $\Delta V$.

4. For a linear elastic soil with shear modulus G, the relationship between p and $(\Delta V/V)$ is

$$(p - \sigma_{ho})/G = -\ell n\ (1 - \Delta V/V) \qquad (2)$$

and this leads to a curve of steadily increasing slope in the $p{:}\ell n\ (\Delta V/V)$ diagram. If cavity pressure p is plotted against cavity strain $\varepsilon_c$ then a straight line relationship is found

$$dp/d\varepsilon_c = 2G \qquad (3)$$

5. During this elastic deformation the mean stress remains constant and the cavity pressure and radial stress are

$$p = \sigma_r = \sigma_{ho} + \tau \qquad (4)$$

while the circumferential stress is

$$\sigma_\theta = \sigma_{ho} - \tau \qquad (5)$$

6. As soon as the soil behaviour at the cavity wall ceases to be elastic then expressions (2) and (3) cease to apply. In the method presented in Ref. 3 for estimating in situ total horizontal stress from Menard pressuremeter tests it is assumed that this occurs when the shear stress $\tau$ at the cavity wall reaches the peak undrained strength $c_u$ of the soil. A precisely similar argument can be used if the soil is assumed to be an elastic–hardening plastic material, and it is this assumption that is made here. The object of both methods is to force the $p{:}\varepsilon_c$ and $p{:}\ell n(\Delta V/V)$ diagrams to be mutually consistent during the elastic response of the soil. This is achieved in practice by identifying one point at which consistency is to be obtained, most conveniently the point at which the behaviour ceases to be elastic. Consistency is obtained by putting the origin for $\Delta V$, and hence by implication the point at which $p = \sigma_{ho}$, in such a place that the slope of the $p{:}\ell n\ (\Delta V/V)$ curve corresponds to the difference $p-\sigma_{ho}$ on the $p{:}\varepsilon_c$ curve. From (1) and (4):

$$p - \sigma_{ho} = dp/d[\ell n(\Delta V/V)] \qquad (6)$$

7. With pressuremeter test results stored on a microcomputer this equation can readily be solved graphically by trial and error on the computer display screen. The correspondence that is sought is illustrated in Fig. 1.

## SELF-BORING PRESSUREMETER TESTS AT ISLINGTON

8. A new station and associated escalator and running tunnels are to be constructed by London Underground at Angel, Islington. Ground movements caused by new construction close to pile foundations and existing tunnels are

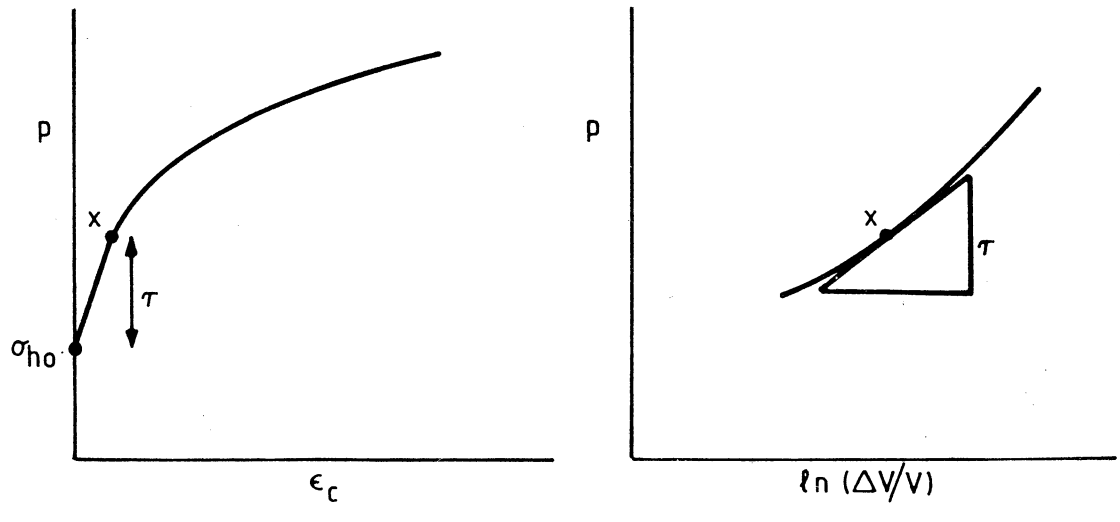


Fig. 1: Diagram of modified Marsland–Randolph method.

of importance, and their prediction requires a good assessment of the in-situ horizontal stress, $\sigma_{ho}$, in the ground, particularly in relation to horizontal movements. This was assessed by recovering high quality samples and measuring suctions in them, and by undertaking self-boring pressuremeter (SBP) tests.

9. A summary of the soil profile at the site is shown in Fig. 2a. Atterberg limits of the London clay and upper strata of the Woolwich and Reading beds clays are plotted on Fig. 2b. 'Undisturbed' soil samples were taken with conventional driven U102 sampling tubes, and also by high quality thin-walled 100 mm dia extruded steel tubes (1.0 m long with end area ratio 9.4%, zero inside clearance and edge taper angle $16^{0}$) which were advanced into the clay by hydraulic rams in one continuous push over a period of 10 mins. The fieldwork and laboratory testing were undertaken by Ground Engineering. Undrained shear strength measurements from triaxial compression tests on specimens from the two types of sample tube are shown on Fig. 2c.

10. Piezometric observations in the immediate area of the site are summarised on Fig. 2d. At depth, the measured pore pressures are significantly lower than the hydrostatic values corresponding to the observed groundwater table at +27 m OD. This is probably a result of pumping from the underlying chalk aquifer (shown on Fig. 2a). Local well records and general patterns of piezometric levels in the London area (Ref. 4) indicate that the current piezometric level in the Chalk and Thanet Sands aquifer at the Islington site is probably about −45 m OD. The pore pressure at the top of the Thanet Sand is therefore likely to be zero, and the assumed profile through the soil strata is shown in Fig. 2d.

11. Suctions in the 100 mm specimens obtained from the thin-walled tube samples were measured using the procedure described in Refs. 5, 6. The $\sigma_{ho}$ values were inferred from the measurements, assuming that the mean effective stress remains constant during sampling and specimen preparation. The corresponding $K_o$ values, assuming the pore pressure profile in Fig. 2d, are shown on Figs. 2 e,f. The results indicate a trend of a low value of $K_o$ down to about 10 m below the top of the London clay, increasing to significantly higher values between 10 m and 15 m, and then decreasing with depth. A single measurement on a sample of the Woolwich and Reading beds clay indicates a $K_o$ value of 0.8, which is similar to the value obtained close to the bottom of the London clay.

12. A profile of SBP tests was undertaken by Cambridge InSitu down to a depth of 23 m below ground level. Measurements of $\sigma_{ho}$ have been interpreted by the lift off method and by the modified Marsland and Randolph approach described above. If the SBP has been carefully calibrated (Ref. 7) and installed with minimal disturbance, the initial response of all three strain arms should in theory be as shown in Fig. 3a; the detection of lift-off is then clear and unambiguous. Unfortunately strain arm responses in stiff clays are often more erratic (Figs. 3b, c, d), in spite of careful attention to calibration, and there may be significant differences between the three strain arms. A reasonably common response is as shown in Fig. 3b; there is then ambiguity as to whether points A or B (or even C) should be taken to correspond to $\sigma_{ho}$. These difficulties are discussed in detail in Ref. 8.

13. Each strain arm response has been separately examined using the lift-off method, and those responses without clearly discernible lift-off points have been rejected. The $K_o$ values obtained are shown in Fig. 2e. Every strain arm response has been interpreted by the modified Marsland and

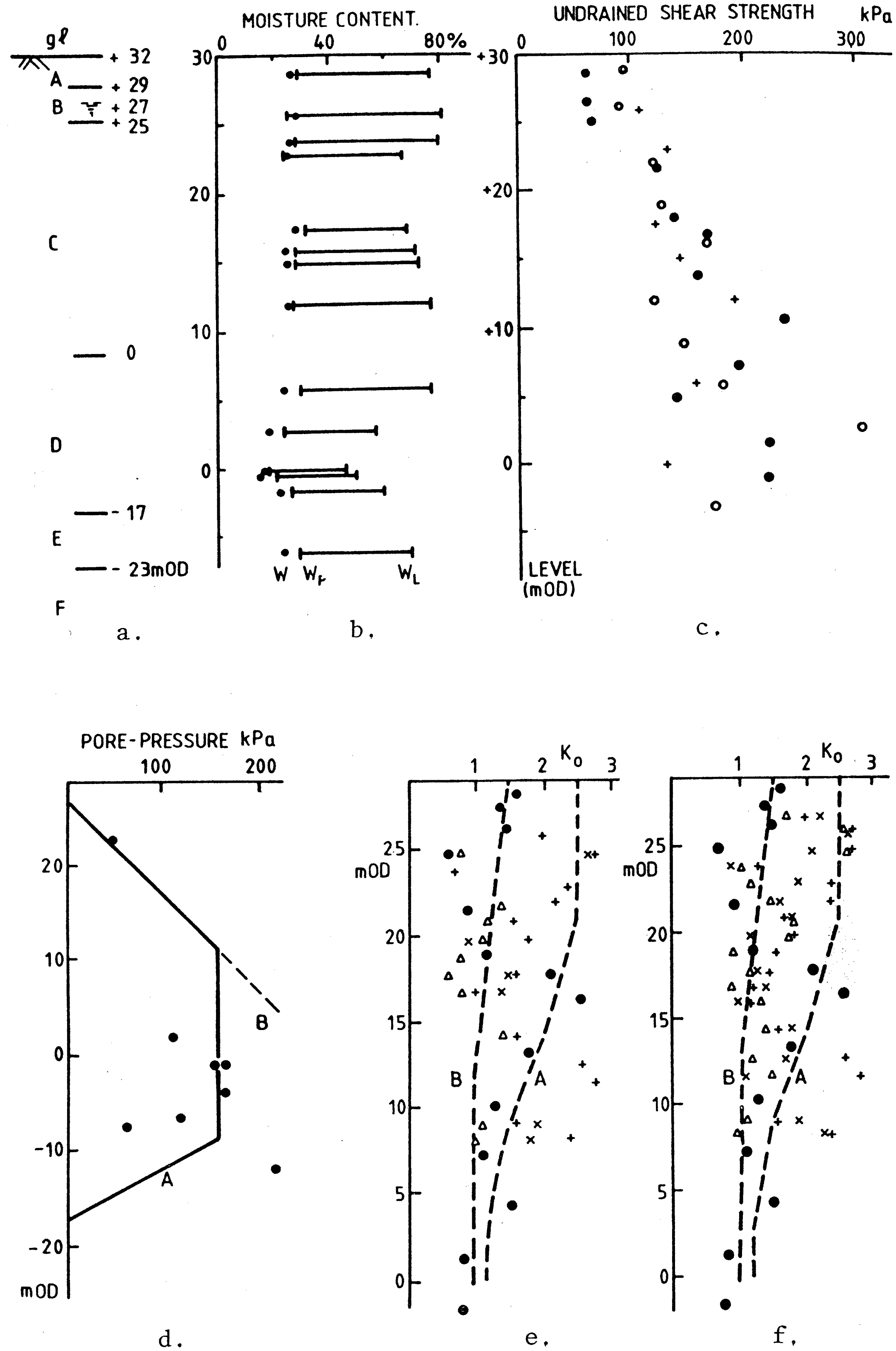


Fig. 2: Angel, Islington (key opposite)

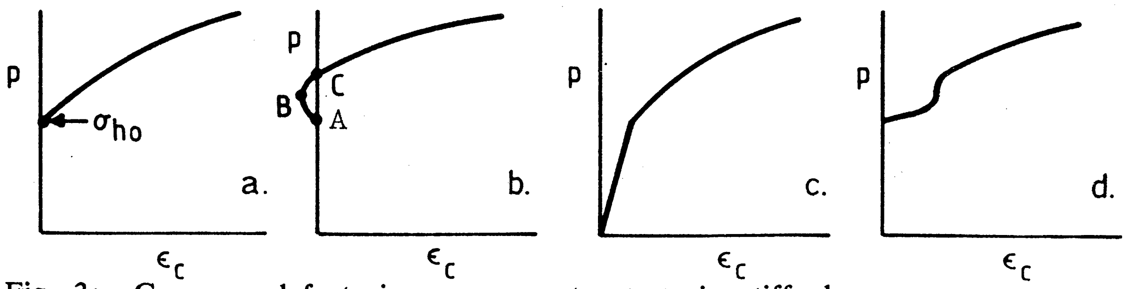


Fig. 3: Common defects in pressuremeter tests in stiff clay.

Randolph approach, and the $K_o$ values thus obtained are shown in Fig. 2f. Although there is a considerable degree of scatter, the SBP results using the two methods of interpretation are broadly consistent, and are reasonably similar to the data from the suction measurements on high quality samples.

14. At a depth of about 16 m below the top of the clay, the SBP encountered claystones and had to be removed so that a shell and auger rig could advance the hole. It is noticeable that the difference between the $K_o$ values inferred from the three strain arms by the modified Marsland and Randolph approach becomes more marked for the remaining tests below 16 m. It is not clear whether this is because one or more of the strain arms apparently measures higher horizontal stresses due to the presence of claystones or locally harder zones, or because there is greater disturbance associated with installation of the SBP in more heterogeneous ground.

## SELF-BORING PRESSUREMETER AND HIGH PRESSURE DILATOMETER TESTS AT FAWLEY

15. As part of the site investigation for a proposed CEGB 1800 MW coal fired power station at Fawley, Hampshire a series of pressuremeter tests were performed by Cambridge In Situ under subcontract to Wimpey Laboratories Ltd. SBP tests were performed in the softer materials until the limit of the device was reached at a depth of 43m; thereafter the Cambridge Insitu Direct Strain Measuring High Pressure Borehole Dilatometer (HPD) was used. This is a Ménard type of pressuremeter (Ref. 7) – the device is lowered into a prebored hole. The tests were carried out to obtain values of shear moduli and undrained shear strength, but it is the results of the in-situ horizontal stress measurement, required for tunnel and shaft lining design that are reported here.

Fig. 2: Angel, Islington.

a. Soil profile (A: made ground; B: brown weathered firm to stiff London clay; C: grey stiff to very stiff London clay; D: brown/red mottled very stiff Woolwich and Reading beds clays; E: very dense Thanet sands; F: chalk);

b. Index properties;

c. Strengths (o : BH A, + : BH B : 100 mm specimens from U102 driven tube; • : BH B : 100 mm specimens from thin-walled tube samples);

d. Pore water pressures (A: assumed pore pressure profile; B: hydrostatic);

e. $\sigma_{ho}$ from suction tests (•) and SBP lift off (+ arm 1, x arm 2, △ arm 3) (A: upper bound for analysis; B: lower bound for analysis);

f. $\sigma_{ho}$ from suction tests (•) and modified Marsland-Randolph method (+ arm 1, x arm 2, △ arm 3) (A: upper bound for analysis; B: lower bound for analysis).

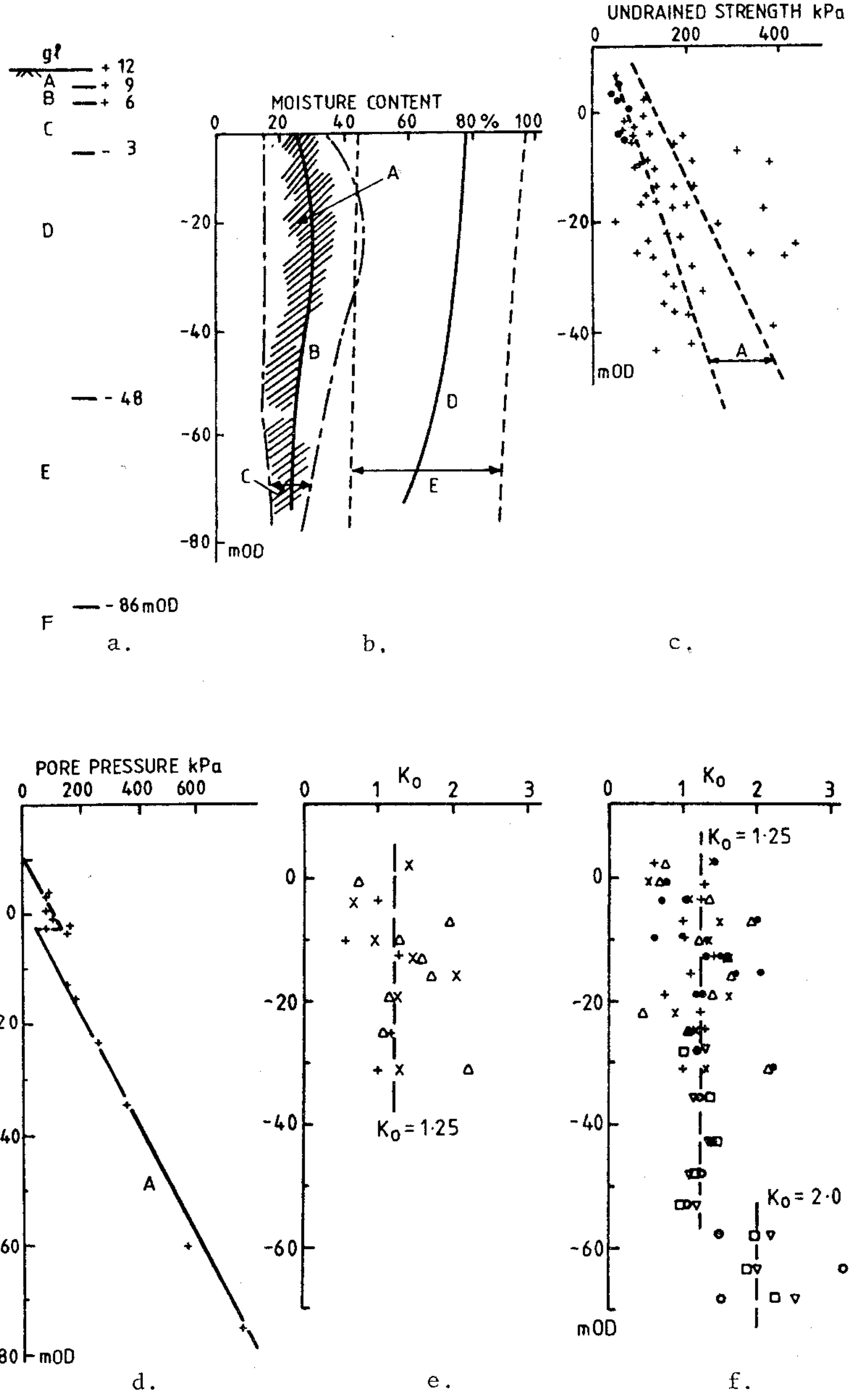


Fig. 4: Fawley (key opposite)

16. A summary of the soil profile at the site is shown in Fig. 4a. Moisture content, plastic and liquid limit profiles for the Barton clay are shown in Fig. 4b. 'Undisturbed' soil samples were taken using conventional driven U102 sampling tubes. The results of single stage 100 mm dia quick undrained triaxial tests and undrained shear strengths determined from standard penetration tests using an empirical correlation $c_u = 4.2N$ (Ref. 9) are shown in Fig. 4c. Undrained shear strengths determined from large diameter plate tests (Ref. 10) are also shown in Fig. 4c.

17. Piezometric measurements from the main site are shown in Fig. 4d indicating non-hydrostatic conditions with depth. It appears that a perched water table exists in the surface gravel and sand layers. The assumed pore pressure profile is shown on Fig. 4d.

18. In situ pressures from SBP tests in borehole P4 from ground level to a depth of 43m are shown in Figs. 4 e,f. In this borehole there is a short overlap section where the SBP and the HPD were used alternately. It was found at this site too that the strain arm response in these stiff clays was erratic, and significant differences could occur in the behaviour of the three strain arms. The values of $K_o$ deduced from acceptable lift-off observations are shown in Fig. 4e. Values of $K_o$ have also been estimated using the modified Marsland and Randolph method and these are plotted in Fig. 4f together with the spread of data from the lift-off measurements.

19. HPD tests were performed between depths of 40 m and 80 m below ground levels. Deformations of the soil are measured directly by means of linear transducers inside the expanding cavity, but because of the disturbance caused during the installation of the pressuremeter it is not possible to interpret lift-off values as being representative of in situ stress conditions. The modified Marsland and Randolph approach can be readily applied to these test data and resulting values of $K_o$ are presented in Fig. 4f. Identification of the yield point can be assisted by examining the 'creep' plot (Ref. 7). It seems that the HPD and SBP measurements are broadly consistent. The reason for the apparently higher values of $K_o$ below −55m OD is not known.

## DISCUSSION

20. Equations (4) and (5) only apply while the soil is behaving elastically and this method of choosing an origin is ideal if the variation of tangent stiffness with strain is as shown by the solid line in Fig. 5 – with a sudden drop in stiffness as the initial yield surface is passed. Accurate measurements of stiffness of soils made in triaxial tests at Imperial College (Ref. 11)

Fig. 4: Fawley.
a. Soil profile (A: sandy gravel; B: fine silty sand; C: firm to stiff sandy silty clay; D: stiff to hard fissured silty clay (Upper Barton clay); E: sandy silty clay (Lower Barton clay); F: very dense fine sand with clay layers (Bracklesham beds/Selsey sands);
b. Index properties (A: range of natural moisture content; B: mean $w_P$; C: range of $w_P$; D: mean $w_L$; E: range of $w_L$);
c. Strengths (● large diameter plate tests; + UU triaxial; A: SPT range);
d. Pore water pressures (A: assumed pore pressure profile);
e. $\sigma_{ho}$ from SBP lift off (+ arm 1, x arm 2, △ arm 3);
f. $\sigma_{ho}$ from SBP lift off (●) and modified Marsland–Randolph method (SBP: + arm 1, x arm 2, △ arm 3; HPD: □ arm 1, o arm 2, ▽ arm 3).

16. A summary of the soil profile at the site is shown in Fig. 4a. Moisture content, plastic and liquid limit profiles for the Barton clay are shown in Fig. 4b. 'Undisturbed' soil samples were taken using conventional driven U102 sampling tubes. The results of single stage 100 mm dia quick undrained triaxial tests and undrained shear strengths determined from standard penetration tests using an empirical correlation $c_u = 4.2N$ (Ref. 9) are shown in Fig. 4c. Undrained shear strengths determined from large diameter plate tests (Ref. 10) are also shown in Fig. 4c.

17. Piezometric measurements from the main site are shown in Fig. 4d indicating non-hydrostatic conditions with depth. It appears that a perched water table exists in the surface gravel and sand layers. The assumed pore pressure profile is shown on Fig. 4d.

18. In situ pressures from SBP tests in borehole P4 from ground level to a depth of 43m are shown in Figs. 4 e,f. In this borehole there is a short overlap section where the SBP and the HPD were used alternately. It was found at this site too that the strain arm response in these stiff clays was erratic, and significant differences could occur in the behaviour of the three strain arms. The values of $K_o$ deduced from acceptable lift-off observations are shown in Fig. 4e. Values of $K_o$ have also been estimated using the modified Marsland and Randolph method and these are plotted in Fig. 4f together with the spread of data from the lift-off measurements.

19. HPD tests were performed between depths of 40 m and 80 m below ground levels. Deformations of the soil are measured directly by means of linear transducers inside the expanding cavity, but because of the disturbance caused during the installation of the pressuremeter it is not possible to interpret lift-off values as being representative of in situ stress conditions.
The modified Marsland and Randolph approach can be readily applied to these test data and resulting values of $K_o$ are presented in Fig. 4f. Identification of the yield point can be assisted by examining the 'creep' plot (Ref. 7). It seems that the HPD and SBP measurements are broadly consistent. The reason for the apparently higher values of $K_o$ below −55m OD is not known.

## DISCUSSION

20. Equations (4) and (5) only apply while the soil is behaving elastically and this method of choosing an origin is ideal if the variation of tangent stiffness with strain is as shown by the solid line in Fig. 5 – with a sudden drop in stiffness as the initial yield surface is passed. Accurate measurements of stiffness of soils made in triaxial tests at Imperial College (Ref. 11)

Fig. 4: Fawley.
a. Soil profile (A: sandy gravel; B: fine silty sand; C: firm to stiff sandy silty clay; D: stiff to hard fissured silty clay (Upper Barton clay); E: sandy silty clay (Lower Barton clay); F: very dense fine sand with clay layers (Bracklesham beds/Selsey sands);
b. Index properties (A: range of natural moisture content; B: mean $w_P$; C: range of $w_P$; D: mean $w_L$; E: range of $w_L$);
c. Strengths (● large diameter plate tests; + UU triaxial; A: SPT range);
d. Pore water pressures (A: assumed pore pressure profile);
e. $\sigma_{ho}$ from SBP lift off (+ arm 1, x arm 2, △ arm 3);
f. $\sigma_{ho}$ from SBP lift off (●) and modified Marsland–Randolph method (SBP: + arm 1, x arm 2, △ arm 3; HPD: □ arm 1, o arm 2, ▽ arm 3).

suggest that for many clays the relationship between tangent stiffness and strain will be more like the dotted line in Fig 5, so that the truly elastic region is very small. This does not invalidate the method of choice of origin proposed here provided that the elastic region that is identified is this stiff initial truly elastic region.

21. The sub-tangent construction for interpretation of pressuremeter data at small strains shows that in general

$$dp/d\varepsilon_c = 2G_s = \tau/\varepsilon_c \qquad (7)$$

where $G_s$ is the current value of the secant modulus. Even when the soil is not behaving elastically an incremental or tangent shear stiffness $G_t$ can be defined

$$G_t = \frac{1}{2}\, d\tau/d\varepsilon_c \qquad (8)$$

Hence, from (7),

$$G_t = \frac{1}{2}\,(dp/d\varepsilon_c + \varepsilon_c d^2p/d\varepsilon_c{}^2) \qquad (9)$$

Even though the tangent stiffness $G_t$ may fall rapidly when the initial small truly elastic region is left, this has an immediate effect only on the curvature of the $p:\varepsilon_c$ relationship and not on the slope. Close identification of the yield point from the cavity expansion information may not be easy.

22 The data presented in Ref. 11 suggest that the strain level marking the end of the initial high stiffness truly elastic region may be of the order of 0.01% axial strain or even lower in undrained triaxial compression. If it is assumed that stiffness change is governed by octahedral shear strains, this implies a cavity strain of the same order (strictly increased by a factor $2/\surd3$) in the pressuremeter tests. Such strains are smaller than can be reliably observed with existing pressuremeter equipment. It is unlikely that field test conditions could ever be so carefully controlled that such resolutions could become credible.

23. The initial stiffnesses being suggested in Ref. 11 are extremely high and the strains involved during cavity expansion are likely to be of the same order as the membrane and transducer corrections that have to be applied. As a result the detection of lift-off, even in a perfectly performed test, may not be straightforward.

24. Actual test data do not follow the ideal pattern shown in Fig. 1 and it is inevitable that the "elastic" stage that is identified will contain experimental points lying scattered about an ideal relationship. The consequence of the

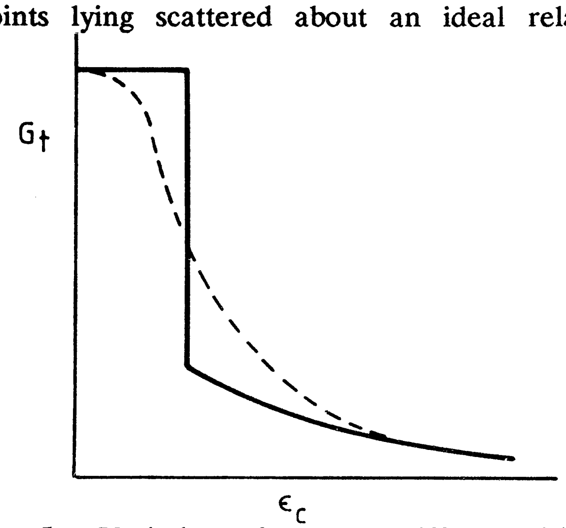


Fig. 5: Variation of tangent stiffness with strain.

fall of stiffness with strain shown in Fig. 5 will be that the average stiffness identified by best fit in this initial region will underestimate the truly elastic high initial stiffness of the soil, and hence that the shear stress $\tau$ will be underestimated and the in situ horizontal total stress $\sigma_{ho}$ from (4) overestimated. This effect may partly explain why profiles of $K_o$ deduced from pressuremeter tests often appear high by comparison with accepted notions of in situ effective stress conditions.

## CONCLUSION

26. The determination of in situ horizontal total stress $\sigma_{ho}$ from pressuremeter tests remains problematic. Examples of the use of the lift-off method and a modified Marsland and Randolph method have been presented here. These two methods represent the best methods available for interpretation of pressuremeter tests, but care is certainly needed in the interpretation and application to design of values of in situ horizontal stress deduced from pressuremeter tests.

## ACKNOWLEDGEMENTS

Data have been presented here by kind permission of London Underground Ltd. and CEGB.

## REFERENCES

1. Palmer, A.C. Undrained plane-strain expansion of a cylindrical cavity in clay: a simple interpretation of the pressuremeter test. Géotechnique 1972 22 3, 451-457.
2. Prévost, J.H. Undrained stress-strain-time behaviour of clays. Proc. ASCE 1976 102 GT 12, 1245-1259.
3. Marsland, A. and Randolph, M.F. Comparisons of the results from pressuremeter tests and large in situ plate tests in London clay. Géotechnique 1977 27 2, 217-243.
4. Chisholm, F.A. Rising groundwater levels under Greater London and their geotechnical significance. M.Sc thesis, University of London (Imperial College) 1984.
5. Skempton, A.W. Horizontal stresses in an overconsolidated Eocene clay. Proc. 5th Int. Conf. Soil Mechs., Paris 1961 1 351-357.
6. Burland, J.B. and Maswoswe, J. Discussion: In situ measurement of horizontal stress in overconsolidated clay using push-in spade-shaped pressure cells. Géotechnique 1982 32 3, 285-286.
7. Mair, R.J. and Wood, D.M. Pressuremeter testing: Methods and interpretation. CIRIA Ground Engineering Report: In-situ testing, CIRIA and Butterworths 1987.
8. Corke, D.J. In situ lateral stress assessment in London clay with the self-boring pressuremeter. Proc. Conf. of Eng. Group of the Geol. Soc., Sunderland 1988.
9. Stroud, M.A. and Butler, F.G. The standard penetration test and the engineering properties of glacial material. Proc. Symp. on the Engineering behaviour of glacial materials. University of Birmingham 124-135.
10. Marsland, A. Large in-situ tests to measure the properties of stiff fissured clays. Proc 1st ANZ Conf. on Geomechs, Melbourne 1971 1 180-189.
11. Jardine, R.J., Symes, M.J. and Burland, J.B. The measurement of soil stiffness in the triaxial apparatus. Géotechnique 1984 34 3, 323, 340.